Designing Patchy Interactions to Self-Assemble Arbitrary Structures

Flavio Romano,[1,2] John Russo,[1,3] Lukáš Kroc,[4] and Petr Šulc[1,4,*]

[1]*Dipartimento di Scienze Molecolari e Nanosistemi, Università Ca' Foscari di Venezia Campus Scientifico, Edificio Alfa, via Torino 155, 30170 Venezia Mestre, Italy*

[2]*European Centre for Living Technology (ECLT) Ca' Bottacin, 3911 Dorsoduro Calle Crosera, 30123 Venice, Italy*

[3]*Dipartimento di Fisica, Sapienza Università di Roma, Piazzale le Aldo Moro 5, 00185 Rome, Italy*

[4]*School of Molecular Sciences and Center for Molecular Design and Biomimetics, The Biodesign Institute, Arizona State University, 1001 South McAllister Avenue, Tempe, Arizona 85281, USA*

(Received 19 April 2020; revised 21 June 2020; accepted 10 August 2020; published 10 September 2020)

One of the fundamental goals of nanotechnology is to exploit selective and directional interactions between molecules to design particles that self-assemble into desired structures, from capsids, to nanoclusters, to fully formed crystals with target properties (e.g., optical, mechanical, etc.). Here, we provide a general framework which transforms the inverse problem of self-assembly of colloidal crystals into a Boolean satisfiability problem for which solutions can be found numerically. Given a reference structure and the desired number of components, our approach produces designs for which the target structure is an energy minimum, and also allows us to exclude solutions that correspond to competing structures. We demonstrate the effectiveness of our approach by designing model particles that spontaneously nucleate milestone structures such as the cubic diamond, the pyrochlore, and the clathrate lattices.

DOI: 10.1103/PhysRevLett.125.118003

Self-assembly is a broad category of processes by which elementary components organize themselves into ordered structures [1]. Inspired by its ubiquity in biology, nanotechnology has long looked at self-assembly as the most promising avenue for the bottom-up realization of structures with specific properties. Successful experimental examples include two-dimensional lattices [2], fully three-dimensional crystals [3,4], and polyhedral shells [5–7]. On the molecular scale, perhaps the most successful results were obtained using DNA nanotechnology, where DNA sequences are designed so that they form the maximum number of base pairs only by self-assembling into the desired target 2D or 3D shape, e.g., DNA origami [8]. Very recently, DNA origami have been crystallized into three-dimensional superlattices [9,10]. At the colloidal scale, promising strategies for self-assembly include DNA-functionalized particles and patchy particles. In the former case, a mixture is obtained from colloids whose surface is randomly decorated with single strands of DNA such that particles of different types can selectively bind to each other. This strategy has led to the self-assembly of the double diamond (or B32) crystal [11]. In the case of patchy particles, colloidal particles acquire anisotropic interactions either via their shape [12] or via chemical patterning of their surface [13–16]. Hybrid solutions where patchy interactions are realized by attaching DNA sequences at well-defined positions have also been proposed [17–20].

The experimental methodologies so far described, while successful, are system specific and hard to generalize. In many cases, we lack a theoretical understanding of why certain structures have self-assembled from elementary building blocks. The search for the general principles behind the inverse self-assembly problem has attracted several theoretical investigations. Instead of predicting which structures self-assemble out of specific building blocks, the inverse problem is concerned with designing building blocks that form a specific target. So far, two types of approaches have emerged: optimization algorithms and geometrical strategies. In optimization algorithms the pair potential is tuned to minimize the energy of a target structure [21–27]. While powerful and general, the major limitation of this approach is that the level of control over the shape of the pair potential is in most cases far beyond current experimental possibilities. The geometric approach to self-assembly instead uses specific interactions to match the geometrical properties of the target structure to kinetically guide the assembly process. The following interaction properties are usually tuned to match the target structure: shape [28], directionality [29–32], selective binding [33], and torsional interactions between neighbors [34,35]. Geometrical approaches allow experimentally realizable systems to self-assemble into specific structures, but the process of designing the potential is system specific and requires *ad hoc* solutions. An example of these limitations is the self-assembly of the colloidal diamond structure, which usually requires either torsional interactions [34,35] or hierarchical assembly [35–38] to avoid the

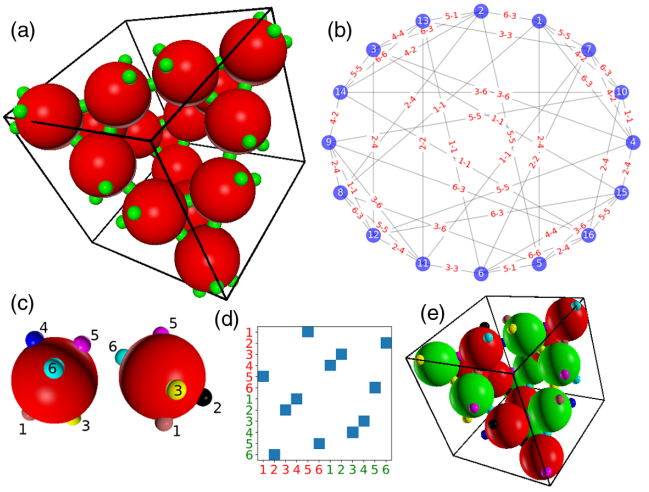

FIG. 1. (a) A schematic representation of the unit cell of a tetrastack lattice consisting of 16 positions (red spheres), each bound to its neighbors (using periodic boundary conditions) via numbered "slots," shown in green. (b) A topology representing the unit lattice, showing each lattice position connected to six other positions (interacting slot numbers on each respective position are shown as link labels). (c) A PP with six patches with each patch colored differently. The PP can be positioned into the lattice so that its patches overlap with the green slots. There are six different orientations that allow us to position a PP into the lattice position so that all patches overlap with the slots. (d) The SAT solver assigns colors to each patch and designs the interaction matrix between the colors. In this particular solution for tetrastack crystal, there are 2 PP species (red and green) with each patch assigned its unique color. The interaction matrix shows which colors interact. (e) The SAT solver assigns to each lattice position a corresponding PP species and an orientation so that all patch interactions are satisfied. Patches that interact with each other are drawn using the same color for convenience.

formation of stacking faults. Importantly, some of these features lack a convincing experimental counterpart.

Here, we formulate a general framework for designing self-assembling systems of patchy particles (PP) into any arbitrary structure, with the option to exclude the formation of competing structures that are identified in simulations. We focus on designing PP systems that have geometric properties, such as the number and placement of the patches that reflect the local environment of the target lattice. To introduce selectivity in the model, we assign to each patch a "color" that encodes its binding properties and define N_c as the number of different patch colors. Binding is allowed only between patches that have compatible colors as specified by an interaction matrix [Fig. 1(d)]. We do not impose any torsional restrictions and all bonds have the same strength. While all particles have the same placement of the patches, we allow for the possibility of having N_s different PP "species," which are defined by the coloring of their patches. Relative concentrations are also free parameters. This system can be realized experimentally with patches based on single-stranded DNA [39] thanks to the selective binding of DNA sequences. To simplify sequence design, we impose that each patch is assigned a color that can only bind one other color (which can be the same in the case of self-complementarity). The goal is to determine the patch coloring for each PP species and color interaction matrix so that the PPs assemble into a desired structure.

The target structure is described by a unit cell, comprising $l \in [1, L]$ particles [Fig. 1(a)]. The unit cell can be a combination of two or more true unit cells of the target lattice. The positions of the patches in the target lattice (slots) are labeled as $k \in [1, N_p]$, from which a list of neighboring slots is computed [Fig. 1(b)]. Our designed PPs can be of different species $s \in [1, N_s]$, and have $p \in [1, N_p]$ patches on their surface which can take a color $c \in [1, N_c]$. o represents one of the N_o possible orientations of each particle, and it is uniquely identified by a map between its patches and the patch slots they occupy. Not all mappings are possible, only those that can be reached by a physical rotation of the particle.

A brute-force search of all possible combinations of (i) patch color arrangements for all particle species $\binom{N_c N_s}{N_p}$, (ii) rotations and symmetry operations of each particle up to $N_p^L!$, and (iii) interaction matrix between patch colors, $\binom{(N_c+1)/2}{N_c}$, becomes intractable with increasing N_c, N_s, N_p, and L even if they are relatively small. Instead, and this a crucial contribution of this Letter, we map the problem to a Boolean satisfiability problem (SAT), where recent algorithmic developments have dramatically advanced our ability to solve problems involving tens of thousands of variables and millions of constraints [40–43]. We use a publicly available SAT solver [40] that can find solutions to the design problems considered here in time ranging from few seconds up to one hour.

Mapping the particle design onto a SAT problem requires the definition of (i) binary variables x_i that describe the PPs' patch coloring for each particle species and the color interaction matrix and (ii) binary clauses C_j that represent the constraints that the variables need to satisfy, such as the ability to form all the bonds in the target lattice. Each binary clause contains a subset of the variables x_i (or their negation $\neg x_i$) connected by an OR statement, and a solution is found whenever a combination of values of the x_i satisfies all clauses at the same time. Formally, this corresponds to finding a set of variables x_i such that $C_1 \wedge C_2 \wedge C_3 \wedge \cdots$ is true. The SAT mapping can also be used to prove the impossibility of achieving some (desired or unwanted) binding pattern with a given combination of input parameters N_s and N_c by proving the absence of solutions to the associated SAT problem. This is crucial since it allows us to filter undesired binding patterns, which may represent competing global arrangements (i.e., another crystal form) or local arrangements (kinetic traps).

TABLE I. SAT clauses and variables. The color interaction is given by binary variables $x^{\text{int}}_{c_i,c_j}$ which are 1 if color c_i is compatible with color c_j and 0 otherwise. The patch coloring for each PP species is described by binary variables $x^{p\text{col}}_{s,p,c}$ which are 1 if patch p of species s has color c, and 0 otherwise. The arrangement of the particle species in the lattice is described by $x^{L}_{l,s,o}$ which is 1 if the position l is occupied by a PP of species s in the specific orientation o. The mapping $\phi_o(k) = p$ for a given orientation o means that PP's patch p overlaps with slot k in a given lattice position. The variable $x^{A}_{l,k,c}$ is 1 if slot k of lattice position l is occupied by a patch with color c and 0 otherwise. The clauses and variables are defined for all possible combinations of colors $c \in [1, N_c]$, patches $p \in [1, N_p]$, slots $k \in [1, N_p]$, PP species $s \in [1, N_s]$, orientations $o \in [1, N_o]$, and lattice positions $l \in [1, L]$. Clauses C^{lint} are defined only for slots k_i, k_j that are in contact in neighboring lattice positions l_i, l_j. For a given s, clause $C^{\text{all}s}_{s}$ is defined as a list of $x^{L}_{l,s,o}$ for all possible values of l and o, joined by disjunctions. Clause $C^{\text{all}c}_{c}$ is defined analogously.

Id	Clauses	Boolean expression
(i)	$C^{\text{int}}_{c_i,c_j,c_k}$	$\neg x^{\text{int}}_{c_i,c_j} \vee \neg x^{\text{int}}_{c_i,c_k}$
(ii)	$C^{p\text{col}}_{s,p,c_k,c_l}$	$\neg x^{p\text{col}}_{s,p,c_k} \vee \neg x^{p\text{col}}_{s,p,c_l}$
(iii)	$C^{L}_{l,s_i,o_i,s_j,o_j}$	$\neg x^{L}_{l,s_i,o_i} \vee \neg x^{L}_{l,s_j,o_j}$
(iv)	$C^{\text{lint}}_{l_i,k_i,l_j,k_j,c_i,c_j}$	$(x^{A}_{l_i,k_i,c_i} \wedge x^{A}_{l_j,k_j,c_j}) \Rightarrow x^{\text{int}}_{c_i,c_j}$
(v)	$C^{\text{LS}}_{l,s,o,c,k}$	$x^{L}_{l,s,o} \Rightarrow (x^{A}_{l,k,c} \Leftrightarrow x^{p\text{col}}_{s,\phi_o(k),c})$
(vi)	$C^{\text{all}s}_{s}$	$\bigvee_{\forall\, l,o} x^{L}_{l,s,o}$
(vii)	$C^{\text{all}c}_{c}$	$\bigvee_{\forall\, s,p} x^{p\text{col}}_{s,p,c}$

Our design problem thus translates into a set of binary variables and clauses, as defined in Table I. In order, the clauses enforce that (i) C^{int}: each color is compatible with exactly one color, (ii) $C^{p\text{col}}$: each patch is assigned exactly one color, (iii) C^{L}: each lattice position is occupied by a single PP species with one assigned orientation, (iv) C^{lint}: colors of patches that interact in the target lattice can bind to each other according to the interaction matrix, (v) C^{LS}: the slots in each lattice position are set to have the color of the patch occupying them, (vi) $C^{\text{all}s}_{s}$: all N_s particle species are used for the lattice assembly, (vii) $C^{\text{all}c}$: all N_c patch colors are used in the solution. The final SAT problem is a conjunction of all clauses (i)–(vii). The conditions (vi) and (vii) are used to avoid getting trivial solutions such as having a single PP species with all patches colored by the same self-complementary color. It allows us to formulate the SAT problems for different combinations of N_s and N_c and see for which the solutions exist.

For the lattice design problems considered in this work, the number of binary variables ranges from about 10^3 to 10^5, and the number of clauses ranges from approximately 10^4 to 10^7, which we found to be within reach of a commonly used SAT solver [40]. If a solution is found in terms of the binary variables x, it can be straightforwardly converted into human-readable form by listing the variables $x^{p\text{col}}_{s,p,c}$ and $x^{\text{int}}_{c_i,c_j}$ that are 1, as their subscripts will specify respectively (i) the color c of patch p in PP species s, (ii) the compatible colors c_i and c_j. Additionally, our framework allows the user to quickly check if a specific combination of PP species with a patch coloring and color interaction matrix can satisfy a given lattice geometry. We use clauses (i)–(iv) discussed above, and additionally add clauses that constrain the variables $x^{p\text{col}}$ and x^{int} accordingly for the set of PPs we want to check. If such a SAT problem is solvable, the indices of the variables $x^{L}_{l,s,o}$ that are 1 readily provide the particle species s and orientation o assigned to each lattice position l, allowing visualization of the lattice [Fig. 1(e)].

To demonstrate the versatility of the SAT mapping approach for particle design, we selected three of the most challenging and sought-after lattice geometries. After using our SAT solver to obtain PP species design and color interaction matrix, we run molecular simulations [44] and study the success and quality of the crystals obtained from homogenous nucleation. The SAT solver guarantees that the target structure is an energy minimum, but cannot say whether kinetic traps or other energy minima, both often associated with competing crystalline structures, are present along the self-assembly pathway. If a competing structure is found in the molecular simulations, we can explicitly exclude it by redesigning the SAT problem by adding additional clauses or by discarding all generated solutions that can form the identified undesired structures. Thus we iteratively arrive at a design which self-assembles into the desired crystal through homogeneous nucleation. In contrast to previous solutions to this problem, we stress that these crystalline structures are being nucleated without introducing torsional interactions or hierarchical assembly. Moreover, the crystals are nucleated homogeneously, without the need for seeding or templating, and grow without stacking defects.

Our first target structure is the cubic tetrastack lattice (also known as pyrochlore) that together with the cubic diamond has been proposed for its omnidirectional photonic band gap for use as a photonic crystal [45]. We adopt a design with six patches in the direction of the closest neighbors [Figs. 1(a) and 1(c)]. To mimic the possible experimental realization of the system using 3D DNA nanostructures [46], with single-stranded DNA representing individual patches, we model the PPs as soft spheres with attractive point patches (as described in Supplemental Material [47]). Solutions can be found with $N_s = 1$, $N_c = 3$ but suffer from the geometric problem in which two particles can bind with two bonds at the same time, leading to alternative assemblies in the simulations. To avoid this we introduced an additional clause (defined in the Supplemental Material [47]) that requires that no pair of particles can bind through more than one bond. This SAT

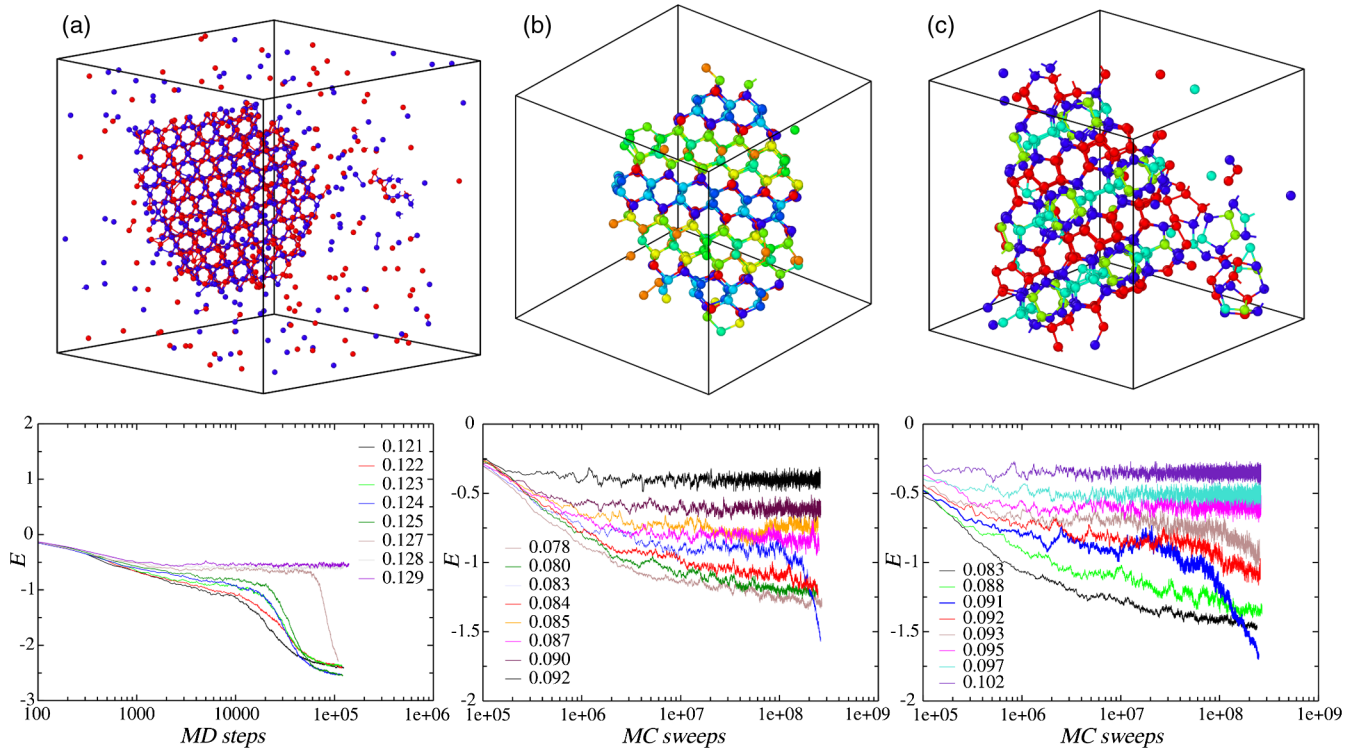

FIG. 2. Overview of simulations of the assembly of (a) tetrastack, (b) diamond cubic, and (c) clathrate Si34 lattices. Top panels show a snapshot of the final configuration of simulations that nucleated a crystal assembly, with each particle species colored differently. Patches are not shown for clarity. The bottom row shows the energy per particle over the course of the simulations at different temperatures, where nucleation events are signaled by sudden drops in E. For tetrastack, we saw multiple independent nucleations for $T < 0.127$. Energy is reported in simulation energy unit ϵ^* and temperature is in ϵ^*/k_B.

problem has no solution for $N_s = 1$. For $N_s = 2$, we found solutions for $N_c = 6$, 8, 10, and 12. We show the solution for $N_c = 12$ in Figs. 1(d) and 1(e) and its successful nucleation in Fig. 2(a). To simulate the assembly kinetics, we used simulations at a range of temperatures of a point-patch-particle model [49] (see the Supplemental Material [47] for model and simulation details). The simulations were carried out with 2048 particles at number density 0.1 (corresponding to a volume fraction of ≈0.05). This density was chosen to mimic the common experimental scenario of phase-separation-induced crystallization from a low-density solution. Figure 2(a) shows a nucleation event: the top panel shows a snapshot of the nucleus, the bottom panel shows the time evolution of the energy for runs at different temperatures, where the nucleating trajectory is signaled by the sharp decrease in energy. We further obtained successful nucleation for $N_c = 8$ and 10, but only observed gas or glassy state for $N_c = 6$ with no crystal nucleation in simulations. The dependence of the phase diagram on N_c will be explored in future work.

We next consider the tetravalent PP assembly. One of the most popular models for the study of tetravalent systems is the Kern-Frenkel (KF) potential [50], which is a square-well potential with angular dependence (see Supplemental Material [47]). The thermodynamic and crystallizability of the model have been well characterized [44,51], and have highlighted the difficulty of obtaining nucleations of a pure crystal due to the many kinetic traps represented by competing structures. Because of the discontinuous nature of the potential, the Monte Carlo (MC) method is commonly employed to study its assembly [44,52,53]. In the following, we hence adopt MC to identify alternative stable or metastable structures competing with the desired target tetravalent lattice.

We seek the assembly of the cubic diamond (DC) lattice, probably the most sought-after crystal for photonic applications [54]. Systems that can assemble DC lattice are almost inevitably found to be also able to assemble into hexagonal diamond (HD) lattice [51], resulting in imperfect crystals with defects and stacking faults. We adopted a tetrahedral PP design ($N_p = 4$), and we looked for solutions that color an 8-particle unit cell of DC but cannot color a 8-particle unit cell of HD. Even in this case, our SAT solver showed that any PP solution that satisfies 8-particle DC cell can also assemble a 32-particle HD unit cell. A strategy to avoid the HD lattice in this case is to employ a larger unit cell for the DC. We hence used a larger 16-particle unit cell of a DC lattice and scanned a range of combinations of $N_s > 8$ and N_c. For each solution that we obtained for a given N_s and N_c, we checked with the SAT

solver if it can assemble into a 32-particle HD unit cell. The solution with the smallest N_s that we found to be able to form DC and not form 32-particle HD cell had $N_s = 9$ and $N_c = 31$, and it successfully nucleated the DC lattice in a Kern-Frenkel PP [51] simulation [Fig. 2(b)], which was done with 495 particles split equally into 9 PP species, at number density 0.2 (corresponding to volume fraction 0.1). We have also carried out simulations at 0.1 number density with 2048 particles, which also showed homogeneous nucleation of a DC lattice (shown in the Supplemental Material [47]).

As the last example, we used our approach to find a system able to nucleate into the Si34 clathrate (CSi34) starting from tetrahedral PPs in the KF model. The smallest N_s for which a solution was found that could form CSi34 and not DC or HD lattices had $N_s = 4$, $N_c = 12$, and was confirmed to successfully nucleate CSi34 [Fig. 2(c)] in a simulation at 0.2 number density with 476 particles in species ratio 6:3:2:6, as well as in a larger simulation at number density 0.1 and 1904 particles (shown in the Supplemental Material).

The patch coloring and interaction matrices for all PP solutions are given in the Supplemental Material [47]. While we focused so far only on designing systems for the assembly of difficult 3D lattices, our approach can be generalized to other systems, such as finite-size clusters. Our method is not limited to spherical PPs and can be used for any model where simulations or other stochastic methods can identify undesired assemblies as a list of interactions between PP species and their patches. It can be also combined with other techniques, such as using different strengths of interactions to disfavor undesired assemblies identified in the simulations. The approach proposed here is extensible and the systems designed in this work should be amenable of experimental realization.

J. R. acknowledges support from the European Research Council Grant No. DLV-759187. P. Š. acknowledges support from the ONR Grant No. N000142012094. J. R. and P. Š. acknowledge support from the Università Ca' Foscari for a Visiting Scholarship.

*Corresponding author.
psulc@asu.edu

[1] S. Whitelam and R. L. Jack, Annu. Rev. Phys. Chem. **66**, 143 (2015).
[2] Q. Chen, S. C. Bae, and S. Granick, Nature (London) **469**, 381 (2011).
[3] J. Chen and N. C. Seeman, Nature (London) **350**, 631 (1991).
[4] S. M. Douglas, H. Dietz, T. Liedl, B. Högberg, F. Graf, and W. M. Shih, Nature (London) **459**, 414 (2009).
[5] N. Takeda, K. Umemoto, K. Yamaguchi, and M. Fujita, Nature (London) **398**, 794 (1999).
[6] D. Bhatia, S. Mehtab, R. Krishnan, S. S. Indi, A. Basu, and Y. Krishnan, Angew. Chem., Int. Ed. Engl. **48**, 4134 (2009).
[7] Y. Liu, C. Hu, A. Comotti, and M. D. Ward, Science **333**, 436 (2011).
[8] P. W. K. Rothemund, Nature (London) **440**, 297 (2006).
[9] W. Liu, M. Tagawa, H. L. Xin, T. Wang, H. Emamy, H. Li, K. G. Yager, F. W. Starr, A. V. Tkachenko, and O. Gang, Science **351**, 582 (2016).
[10] T. Zhang, C. Hartl, K. Frank, A. Heuer-Jungemann, S. Fischer, P. C. Nickels, B. Nickel, and T. Liedl, Adv. Mater. **30**, 1800273 (2018).
[11] Y. Wang, I. C. Jenkins, J. T. McGinley, T. Sinno, and J. C. Crocker, Nat. Commun. **8**, 14173 (2017).
[12] G. van Anders, N. K. Ahmed, R. Smith, M. Engel, and S. C. Glotzer, ACS Nano **8**, 931 (2013).
[13] Z. Zhang and S. C. Glotzer, Nano Lett. **4**, 1407 (2004).
[14] A. B. Pawar and I. Kretzschmar, Macromol. Rapid Commun. **31**, 150 (2010).
[15] E. Bianchi, R. Blaak, and C. N. Likos, Phys. Chem. Chem. Phys. **13**, 6397 (2011).
[16] F. Romano and F. Sciortino, Nat. Mater. **10**, 171 (2011).
[17] K. Suzuki, K. Hosokawa, and M. Maeda, J. Am. Chem. Soc. **131**, 7518 (2009).
[18] J.-W. Kim, J.-H. Kim, and R. Deaton, Angew. Chem., Int. Ed. Engl. **50**, 9185 (2011).
[19] Y. Wang, Y. Wang, D. R. Breed, V. N. Manoharan, L. Feng, A. D. Hollingsworth, M. Weck, and D. J. Pine, Nature (London) **491**, 51 (2012).
[20] L. Feng, R. Dreyfus, R. Sha, N. C. Seeman, and P. M. Chaikin, Adv. Mater. **25**, 2779 (2013).
[21] M. C. Rechtsman, F. H. Stillinger, and S. Torquato, Phys. Rev. Lett. **95**, 228301 (2005).
[22] E. Marcotte, F. H. Stillinger, and S. Torquato, Soft Matter **7**, 2332 (2011).
[23] E. Marcotte, F. H. Stillinger, and S. Torquato, J. Chem. Phys. **138**, 061101 (2013).
[24] G. Zhang, F. H. Stillinger, and S. Torquato, Phys. Rev. E **88**, 042309 (2013).
[25] M. Z. Miskin, G. Khaira, J. J. de Pablo, and H. M. Jaeger, Proc. Natl. Acad. Sci. U.S.A. **113**, 34 (2016).
[26] D. Chen, G. Zhang, and S. Torquato, J. Phys. Chem. B **122**, 8462 (2018).
[27] R. Kumar, G. M. Coli, M. Dijkstra, and S. Sastry, J. Chem. Phys. **151**, 084109 (2019).
[28] É. Ducrot, M. He, G.-R. Yi, and D. J. Pine, Nat. Mater. **16**, 652 (2017).
[29] D. R. Nelson, Nano Lett. **2**, 1125 (2002).
[30] V. N. Manoharan, M. T. Elsesser, and D. J. Pine, Science **301**, 483 (2003).
[31] Z. Zhang, A. S. Keys, T. Chen, and S. C. Glotzer, Langmuir **21**, 11547 (2005).
[32] F. Romano, J. Russo, and H. Tanaka, Phys. Rev. Lett. **113**, 138303 (2014).
[33] J. D. Halverson and A. V. Tkachenko, Phys. Rev. E **87**, 062310 (2013).
[34] F. Romano and F. Sciortino, Nat. Commun. **3**, 975 (2012).
[35] D. F. Tracey, E. G. Noya, and J. P. K. Doye, J. Chem. Phys. **151**, 224506 (2019).
[36] D. Morphew, J. Shaw, C. Avins, and D. Chakrabarti, ACS Nano **12**, 2355 (2018).

[37] N. Patra and A. V. Tkachenko, Phys. Rev. E **98**, 032611 (2018).
[38] Y. Ma and A. L. Ferguson, Soft Matter **15**, 8808 (2019).
[39] Y. Tian, J. R. Lhermitte, L. Bai, T. Vo, H. L. Xin, H. Li, R. Li, M. Fukuto, K. G. Yager, J. S. Kahn *et al.*, Nat. Mater. **19**, 789 (2020).
[40] N. Een and N. Sorensson, in *Proceedings of the SAT-05: 8th International Conference on Theory and Applications of Satisfiability Testing* (Springer-Verlag, Berlin, 2005), pp. 502–518.
[41] J. H. Liang, C. Oh, M. Mathew, C. Thomas, C. Li, and V. Ganesh, in *Theory and Applications of Satisfiability Testing – SAT 2018. Lecture Notes in Computer Science, 10929* (Springer, Cham, 2018), pp. 94–110.
[42] C. H. Papadimitriou, in *Proceedings of the 32nd IEEE Symposium on Foundations of Computer Science* (IEEE, New York, 1991), pp. 163–169.
[43] M. Järvisalo, D. Le Berre, O. Roussel, and L. Simon, AI Magazine **33**, 89 (2012).
[44] L. Rovigatti, J. Russo, and F. Romano, Eur. Phys. J. E **41**, 59 (2018).
[45] T. Ngo, C. Liddell, M. Ghebrebrhan, and J. Joannopoulos, Appl. Phys. Lett. **88**, 241920 (2006).
[46] R. Veneziano, S. Ratanalert, K. Zhang, F. Zhang, H. Yan, W. Chiu, and M. Bathe, Science **352**, 1534 (2016).
[47] See Supplemental Material at http://link.aps.org/supplemental/10.1103/PhysRevLett.125.118003 for description of the models used in simulations, list of solutions found for the studied lattices, and detailed descriptions of all SAT clauses, which also includes Ref. [48].
[48] J. Russo, P. Tartaglia, and F. Sciortino, J. Chem. Phys. **131**, 014504 (2009).
[49] L. Rovigatti, P. Šulc, I. Z. Reguly, and F. Romano, J. Comput. Chem. **36**, 1 (2015).
[50] N. Kern and D. Frenkel, J. Chem. Phys. **118**, 9882 (2003).
[51] F. Romano, E. Sanz, and F. Sciortino, J. Chem. Phys. **134**, 174502 (2011).
[52] W. L. Miller and A. Cacciuto, J. Chem. Phys. **133**, 234108 (2010).
[53] E. G. Noya, I. Zubieta, D. J. Pine, and F. Sciortino, J. Chem. Phys. **151**, 094502 (2019).
[54] K. M. Ho, C. T. Chan, and C. M. Soukoulis, Phys. Rev. Lett. **65**, 3152 (1990).